

Stellar matter with strong magnetic field within density dependent relativistic models.

A. Rabhi,^{1,2,*} C. Providência,^{1,†} and J. Da Providência^{1,‡}

¹*Centro de Física Teórica, Department of Physics,
University of Coimbra, 3004-516 Coimbra, Portugal*

²*Laboratoire de Physique de la Matière Condensée,
Faculté des Sciences de Tunis, Campus Universitaire, Le Belvédère-1060, Tunisia*

(Dated: November 3, 2018)

The effect of strong magnetic fields on the equation of state (EoS) for compact stars described with density dependent relativistic hadronic models is studied. A comparison with other mean-field relativistic models is done. It is shown that the largest differences between models occur for low densities and that the magnetic field affects the crust properties of star, namely its extension.

PACS numbers: 26.60.-c 26.60.Kp 97.60.Jd 24.10.Jv

I. INTRODUCTION

The study of very asymmetric nuclear matter is presently an important issue due to the radioactive beams which will be operating in the near future and which will allow the investigation of a region of the nuclear matter phase space inaccessible till recently. Asymmetric nuclear matter is of particular interest for the description of stellar matter of compact stars.

Compact star properties depend a lot on the model used to describe the hadronic equation of state (EoS). In particular relativistic nuclear mean-field models [1, 2] are very popular to describe stellar matter because causality will always be satisfied. The imposition of constraints, both coming from measured star properties or from relativistic heavy ion collisions in the laboratory, is essential to test the different models [3].

Magnetars are neutron stars which may have surface magnetic fields larger than 10^{15} G [4–6] and which were discovered at the x-ray and γ -ray energies (for a review refer [7]). They are identified with the anomalous x-ray pulsars (AXP) and soft γ -ray repeaters. Taking as reference the critical

*Electronic address: rabhi@teor.fis.uc.pt

†Electronic address: cp@teor.fis.uc.pt

‡Electronic address: providencia@teor.fis.uc.pt

field at which the electron cyclotron energy is equal to the electron mass $B_c^e = 4.414 \times 10^{13}$ G we define $B^* = B/B_c^e$. It has been shown by several authors that the magnetic fields larger than $B^* = 10^5$ will affect the EoS of compact stars [8, 9]. In particular field-theoretical descriptions based on the non-linear Walecka model (NLWM) [1] were used and several parametrisations compared and it was shown that they had an overall similar behaviour. Very strong magnetic fields can only occur in very young compact stars before the magnetic field has decayed. Recently it was shown [10] from a 2D calculation of the cooling of magnetized stars that the magnetic fields and Joule heating have an important effect of maintaining compact stars warm for a longer time. This kind of simulations need the EoS of the crust. It is, therefore, important to make a study that shows when should the magnetic field be taken into account explicitly in the EoS of the crust. An unstable region in a wider density range will correspond to a larger crust and the properties of the star depending on the crust will be affected. It should, however, be pointed out the estimated surface magnetic fields of detected magnetars is obtained assuming that the lost of angular momentum is entirely due to dipolar radiation of magnetars, and until recently, the strongest estimated magnetic field is of the order of $B^* = 10^2$ and was detected in a quite young star, SGR 1806-20 [11].

At low densities relativistic models with constant coupling parameters have different behaviour from density dependent relativistic hadron models (DDRH) [12, 13]. These models have density dependent coupling parameters and have originally been parametrised so that relativistic Dirac Brueckner Hartree-Fock (DBHF) calculations for nuclear matter were reproduced [14]. Within DDRH models the symmetry energy does not increase linearly with density as parametrizations of the NLWM, like the ones studied in [8], and show a behavior closer to non-relativistic models, either some of the recent parametrizations of the Skyrme interaction like SLy230a [15] or NRAPR [16] or variational microscopic calculations [17]. Since nuclear matter is composed of two different fluids, namely protons and neutrons, the liquid gas phase transition can lead to an isospin distillation phenomenon which has been confirmed experimentally [18]. In [19, 20] it was shown that the distillation effect was described both by NLWM and DDRH models, but DDRH models did not predict an effect so strong as the first ones. Moreover, it was shown that DDRH models have at subsaturation densities a behaviour similar to non-relativistic models, namely models with Skyrme forces [21, 22]. We would like to test these models under different conditions namely β -equilibrium matter under strong magnetic fields. Stellar matter, as found in compact stars, under strong magnetic fields has already been studied before by many authors [8, 9, 23, 24].

The authors of Ref. [25, 26] have stressed the importance of including the scalar isovector virtual $\delta(a_0(980))$ field in hadronic effective field theories when asymmetric nuclear matter is studied.

Its presence introduces in the isovector channel the structure of relativistic interactions, where a balance between a scalar (attractive) and a vector (repulsive) potential exists. The introduction of the δ meson mainly affects the behaviour of the system at high densities, when, due to Lorentz contraction, its contribution is reduced, leading to a harder EoS at densities larger than $\sim 1.5 \rho_0$ [26]. In [27] the effect of this meson on the properties of compact stars were studied and it was shown that the EoS of hadronic matter would become stiffer with its presence. In relativistic models there is a proton-neutron mass splitting only if the scalar isovector δ -meson is included. This occurs for the DDRH δ parametrization we consider. For this model $M_n^* < M_p^*$ in neutron rich nuclear matter [28]. A similar behavior is predicted by the Skyrme interaction SLy230a but an opposite behavior is obtained with other parametrizations of the Skyrme interaction [29]. In a recent work [30] the behavior of the proton-neutron mass splitting in different relativistic nuclear models was analysed and it was shown that some point-coupling models without mesons [31] predict larger neutron masses in neutron rich matter. The proton-neutron mass splitting is a present topic of discussion and the forecoming experiments with radioactive beams will allow the clarification of this point. We will investigate whether this mass splitting has some effect on stellar matter with strong magnetic fields.

In the present paper we will study the behaviour of stellar matter described within DDRH, both with [32] and without [13] the isovector-scalar δ -meson, under very strong magnetic fields. The results are compared with previously studied models, the parametrizations GM3 [33] and TM1 [34] of NLWM. These two models including strong magnetic fields, have been discussed in [8] and [23].

In section II we make a brief review of the model and EoS under the effect of a magnetic field. In section III the formalism is generalised to include the δ -meson. Results are discussed in section IV and conclusions are drawn in section V.

II. THE FORMALISM

For the description of the EoS of neutron star matter, we employ a field-theoretical approach in which the baryons (neutrons, n, and protons, p) interact via the exchange of $\sigma - \omega - \rho$ mesons in the presence of a uniform magnetic field B along the z -axis. The Lagrangian density of the relativistic TW model [12, 13] can be written as

$$\mathcal{L} = \sum_{b=n,p} \mathcal{L}_b + \mathcal{L}_m + \sum_{l=e,\mu} \mathcal{L}_l \quad (1)$$

The baryons ($b=n, p$), leptons ($l=e, \mu$), and mesons (σ, ω and ρ) Lagrangians are given by

$$\begin{aligned}
\mathcal{L}_b &= \bar{\Psi}_b \left(i\gamma_\mu \partial^\mu - q_b \gamma_\mu A^\mu - m_b + \Gamma_\sigma \sigma - \Gamma_\omega \gamma_\mu \omega^\mu - \frac{1}{2} \Gamma_\rho \tau_{3b} \gamma_\mu \rho^\mu - \frac{1}{2} \mu_N \kappa_b \sigma_{\mu\nu} F^{\mu\nu} \right) \Psi_b \\
\mathcal{L}_l &= \bar{\psi}_l (i\gamma_\mu \partial^\mu - q_l \gamma_\mu A^\mu - m_l) \psi_l \\
\mathcal{L}_m &= \frac{1}{2} \partial_\mu \sigma \partial^\mu \sigma - \frac{1}{2} m_\sigma^2 \sigma^2 + \frac{1}{2} m_\omega^2 \omega_\mu \omega^\mu - \frac{1}{4} \Omega^{\mu\nu} \Omega_{\mu\nu} \\
&\quad - \frac{1}{4} F^{\mu\nu} F_{\mu\nu} + \frac{1}{2} m_\rho^2 \rho_\mu \rho^\mu - \frac{1}{4} P^{\mu\nu} P_{\mu\nu}
\end{aligned} \tag{2}$$

where Ψ_b and ψ_l are the baryon and lepton Dirac fields, respectively. The nucleon mass and isospin projection for the proton and neutrons are denoted by m_b and $\tau_{3b} = \pm 1$, respectively. The mesonic and electromagnetic field strength tensors are given by their usual expressions: $\Omega_{\mu\nu} = \partial_\mu \omega_\nu - \partial_\nu \omega_\mu$, $P_{\mu\nu} = \partial_\mu \rho_\nu - \partial_\nu \rho_\mu$, and $F_{\mu\nu} = \partial_\mu A_\nu - \partial_\nu A_\mu$. The nucleon anomalous magnetic moments are introduced via the coupling of the baryons to the electromagnetic field tensor with $\sigma_{\mu\nu} = \frac{i}{2} [\gamma_\mu, \gamma_\nu]$ and strength κ_b with $\kappa_n = -1.91315$ for the neutron and $\kappa_p = 1.79285$ for the proton, respectively. The electromagnetic field is assumed to be externally generated (and thus has no associated field equation), and only frozen-field configurations will be considered. The density dependent strong interaction couplings are denoted by Γ , the electromagnetic couplings by q and the nucleon, mesons and leptons masses by m . The parameters of the model are the nucleon mass $m_b = 939$ MeV, the masses of mesons m_σ , m_ω , m_ρ and the density dependent coupling parameters which are adjusted in order to reproduce some of the nuclear matter bulk properties and relations with DBHF calculations [14], using the following parametrisation

$$\Gamma_i(\rho) = \Gamma_i(\rho_{sat}) f_i(x), \quad i = \sigma, \omega \tag{3}$$

with

$$f_i(x) = a_i \frac{1 + b_i (x + d_i)^2}{1 + c_i (x + d_i)^2} \tag{4}$$

where $x = \rho/\rho_{sat}$ and

$$\Gamma_\rho(\rho) = \Gamma_\rho(\rho_{sat}) \exp[-a_\rho(x - 1)], \tag{5}$$

with the values of the parameters m_i , Γ_i , a_i , b_i , c_i and d_i , $i = \sigma, \omega, \rho$ given in [13]. Other possibilities for these parameters are also found in the literature [35].

The field equations of motion follow from the Euler-Lagrange equations. From the Lagrangian density in Eq. (1), we obtain the following meson field equations in the mean-field approximation

$$m_\sigma^2 \langle \sigma \rangle = \Gamma_\sigma (\rho_p^s + \rho_n^s) = \Gamma_\sigma \rho^s \tag{6}$$

$$m_\omega^2 \langle \omega^0 \rangle = \Gamma_\omega (\rho_p^v + \rho_n^v) = \Gamma_\omega \rho^b \tag{7}$$

$$m_\rho^2 \langle \rho^0 \rangle = \frac{1}{2} \Gamma_\rho (\rho_p^v - \rho_n^v) = \frac{1}{2} \Gamma_\rho \rho_3 \tag{8}$$

and the Dirac equations for nucleons and leptons are given by

$$\begin{aligned} & (i\gamma_\mu\partial^\mu - q_b\gamma_\mu A^\mu - (m_b - \Gamma_\sigma\sigma) - \Gamma_\omega\gamma_0\omega^0 \\ & - \frac{1}{2}\Gamma_\rho\tau_{3b}\gamma_0\rho^0 - \gamma_0\Sigma_0^R - \frac{1}{2}\mu_N\kappa_b\sigma_{\mu\nu}F^{\mu\nu})\Psi_b = 0 \end{aligned} \quad (9)$$

$$(i\gamma_\mu\partial^\mu - q_l\gamma_\mu A^\mu - m_l)\psi_l = 0 \quad (10)$$

where the effective baryon masses are given by

$$m_b^* = m_b - \Gamma_\sigma\sigma \quad (11)$$

and ρ^s is the scalar number density. In charge-neutral, β -equilibrated matter, the conditions

$$\mu_n - \mu_p = \mu_e = \mu_\mu, \quad (12)$$

and

$$\rho_p^v = \rho_e^v + \rho_\mu^v \quad (13)$$

should be satisfied.

The energy spectra for protons, neutrons and leptons (electrons and muons) are given by

$$E_{\nu,s}^p = \sqrt{k_z^2 + \left(\sqrt{m_p^{*2} + 2\nu q_p B} - s\mu_N\kappa_p B\right)^2} + \Gamma_\omega\omega^0 + \frac{1}{2}\Gamma_\rho\rho^0 + \Sigma_0^R \quad (14)$$

$$E_s^n = \sqrt{k_z^2 + \left(\sqrt{m_n^{*2} + k_x^2 + k_y^2} - s\mu_N\kappa_n B\right)^2} + \Gamma_\omega\omega^0 - \frac{1}{2}\Gamma_\rho\rho^0 + \Sigma_0^R \quad (15)$$

$$E_{\nu,s}^l = \sqrt{k_z^2 + m_l^2 + 2\nu|q_l|B} \quad (16)$$

where $\nu = n + \frac{1}{2} - \text{sign}(q)\frac{s}{2} = 0, 1, 2, \dots$ enumerates the Landau levels of the fermions with electric charge q , the quantum number s is +1 for spin up and -1 for spin down cases, and the rearrangement term is given by

$$\Sigma_0^R = \frac{\partial\Gamma_\omega}{\partial\rho}\rho_b\omega_0 + \frac{\partial\Gamma_\rho}{\partial\rho}\rho_3\frac{\rho_0}{2} - \frac{\partial\Gamma_\sigma}{\partial\rho}\rho^s\sigma. \quad (17)$$

The expressions of the scalar and vector densities for protons and neutrons are given by [8]

$$\begin{aligned} \rho_p^s &= \frac{q_p B m_p^*}{2\pi^2} \sum_{\nu=0}^{\nu_{\max}} \sum_s \frac{\sqrt{m_p^{*2} + 2\nu q_p B} - s\mu_N\kappa_p B}{\sqrt{m_p^{*2} + 2\nu q_p B}} \ln \left| \frac{k_{F,\nu,s}^p + E_F^p}{\sqrt{m_p^{*2} + 2\nu q_p B} - s\mu_N\kappa_p B} \right|, \\ \rho_n^s &= \frac{m_n^*}{4\pi^2} \sum_s \left[E_F^n k_{F,s}^n - \bar{m}_n^2 \ln \left| \frac{k_{F,s}^n + E_F^n}{\bar{m}_n} \right| \right], \\ \rho_p^v &= \frac{q_p B}{2\pi^2} \sum_{\nu=0}^{\nu_{\max}} \sum_s k_{F,\nu,s}^p, \end{aligned}$$

$$\rho_n^v = \frac{1}{2\pi^2} \sum_s \left[\frac{1}{3} (k_{F,s}^n)^3 - \frac{1}{2} s \mu_N \kappa_n B \left(\bar{m}_n k_{F,s}^n + E_F^{n2} \left(\arcsin \left(\frac{\bar{m}_n}{E_F^n} \right) - \frac{\pi}{2} \right) \right) \right] \quad (18)$$

and the vector densities for leptons are given by

$$\rho_l^v = \frac{|q_l| B}{2\pi^2} \sum_{\nu=0}^{\nu_{\max}} \sum_s k_{F,\nu,s}^l \quad (19)$$

where $k_{F,\nu,s}^p$, $k_{F,\nu,s}^n$ and $k_{F,\nu,s}^l$ are the Fermi momenta of protons, neutrons and leptons, which are related to the Fermi energies E_F^p , E_F^n and E_F^l as

$$\begin{aligned} k_{F,\nu,s}^{p2} &= E_F^{p2} - \left[\sqrt{m_p^{*2} + 2\nu q_p B} - s \mu_N \kappa_p B \right]^2 \\ k_{F,\nu,s}^{n2} &= E_F^{n2} - \bar{m}_n^2 \\ k_{F,\nu,s}^{l2} &= E_F^{l2} - (m_l^2 + 2\nu |q_l| B), \quad l = e, \mu \end{aligned} \quad (20)$$

with

$$\bar{m}_n = m_n^* - s \mu_N \kappa_n B. \quad (21)$$

The summation in ν in the above expressions terminates at ν_{max} , the largest value of ν for which the square of Fermi momenta of the particle is still positive and which corresponds to the closest integer from below defined by the ratio

$$\begin{aligned} \nu_{max} &= \left[\frac{(E_F^i)^2 - m_i^2}{2|q_i| B} \right], \quad \text{leptons} \\ \nu_{max} &= \left[\frac{(E_F^p + s \mu_N \kappa_p B)^2 - m_p^{*2}}{2|q_p| B} \right], \quad \text{protons.} \end{aligned}$$

The chemical potentials of baryons and leptons are defined as

$$\mu_b = E_F^b + \Gamma_\omega \omega^0 + \frac{1}{2} \Gamma_\rho \tau_{3b} \rho^0 + \Sigma_0^R \quad (22)$$

$$\mu_l = E_F^l = \sqrt{k_{F,\nu,s}^{l2} + m_l^2 + 2\nu |q_l| B}. \quad (23)$$

We solve the coupled Eqs. (6)-(13) self-consistently at a given baryon density in the presence of strong magnetic fields. The energy density of neutron star matter is given by (the index "m" refers to matter)

$$\varepsilon_m = \sum_{b=p,n} \varepsilon_b + \sum_{l=e,\mu} \varepsilon_l + \frac{1}{2} m_\sigma^2 \sigma^2 + \frac{1}{2} m_\omega^2 \omega_0^2 + \frac{1}{2} m_\rho^2 \rho_0^2 \quad (24)$$

where the energy densities of nucleons and leptons have the following forms

$$\varepsilon_p = \frac{q_p B}{4\pi^2} \sum_{\nu=0}^{\nu_{\max}} \sum_s \left[k_{F,\nu,s}^p E_F^p + \left(\sqrt{m_p^{*2} + 2\nu q_p B} - s \mu_N \kappa_p B \right)^2 \ln \left| \frac{k_{F,\nu,s}^p + E_F^p}{\sqrt{m_p^{*2} + 2\nu q_p B} - s \mu_N \kappa_p B} \right| \right],$$

$$\begin{aligned}
\varepsilon_n &= \frac{1}{4\pi^2} \sum_s \left[\frac{1}{2} k_{F,s}^n E_F^{n3} - \frac{2}{3} s \mu_N \kappa_n B E_F^{n3} \left(\arcsin \left(\frac{\bar{m}_n}{E_F^n} \right) - \frac{\pi}{2} \right) - \left(\frac{1}{3} s \mu_N \kappa_n B + \frac{1}{4} \bar{m}_n \right) \right. \\
&\quad \left. \left(\bar{m}_n k_{F,s}^n E_F^n + \bar{m}_n^3 \ln \left| \frac{k_{F,s}^n + E_F^n}{\bar{m}_n} \right| \right) \right] \\
\varepsilon_l &= \frac{|q_l| B}{4\pi^2} \sum_{\nu=0}^{\nu_{\max}} \sum_s \left[k_{F,\nu,s}^l E_F^l + (m_l^2 + 2\nu|q_l|B) \ln \left| \frac{k_{F,\nu,s}^l + E_F^l}{\sqrt{m_l^2 + 2\nu|q_l|B}} \right| \right]
\end{aligned} \tag{25}$$

The pressure of the system is obtained from the expression

$$P_m = \sum_i \mu_i \rho_v^i - \varepsilon_m = \mu_n \rho_b - \varepsilon_m \tag{26}$$

where the charge neutrality and β -equilibrium conditions are used to get the last equality. Note that the contribution from electromagnetic fields to the energy density and pressure, $\varepsilon_f = P_f = \frac{B^2}{8\pi}$, should be taken into account in the calculation of the EoS.

III. INCLUDING ISOVECTOR-SCALAR MESONS

To investigate the influence of the δ -meson we have included in the TW model the isovector-scalar meson term [32], which has density dependent coupling parameters. The Lagrangian density reads

$$\mathcal{L} = \sum_{b=n,p} \mathcal{L}'_b + \mathcal{L}'_m + \sum_{l=e,\mu} \mathcal{L}_l, \tag{27}$$

where the baryon ($b=n, p$), lepton ($l=e, \mu$), and meson (σ, ω, ρ and δ) Lagrangian are given by

$$\begin{aligned}
\mathcal{L}'_b &= \mathcal{L}_b + \bar{\Psi}_b \Gamma_\delta \vec{\tau}_b \cdot \vec{\delta} \Psi_b \\
\mathcal{L}'_m &= \mathcal{L}_m + \mathcal{L}_\delta \\
\mathcal{L}_\delta &= \frac{1}{2} \left(\partial_\mu \vec{\delta} \partial^\mu \vec{\delta} - m_\delta^2 \vec{\delta}^2 \right),
\end{aligned} \tag{28}$$

with \mathcal{L}_b and \mathcal{L}_m defined in Eq (2). Γ_δ and m_δ are, respectively, the coupling constant of the δ meson with the nucleons and its mass. For Γ_σ and Γ_ω we take the parametrisations given in Eqs. (3) and (4). For Γ_ρ and Γ_δ , we use the parametrisation [36]

$$\Gamma_i(\rho) = \Gamma_i(\rho_{sat}) f_i(x), \quad x = \frac{\rho}{\rho_{sat}} \tag{29}$$

with

$$f_i(x) = a_i \exp[-b_i(x-1)] - c_i(x-d_i), \quad i = \rho, \delta \tag{30}$$

and the parameters a_i , b_i , c_i and d_i defined in Table I.

i	Γ_i	a_i	b_i	c_i	d_i
ρ	11.727	0.095268	2.171	0.05336	17.8431
δ	7.58963	0.01984	3.4732	-0.0908	-9.811

TABLE I: Parameters of the DDRH δ model.

From the Lagrangian density in Eq. (27), we obtain the meson field equations (6), (7), (8) plus an equation for the δ -meson in the mean-field approximation

$$m_\delta^2 \langle \delta_3 \rangle = \Gamma_\delta (\rho_p^s - \rho_n^s) = \Gamma_\delta \rho_3^s \quad (31)$$

and the Dirac equations for nucleons are given by

$$\left(i\gamma_\mu \partial^\mu - q_b \gamma_\mu A^\mu - (m_b - \Gamma_\sigma \sigma - \Gamma_\delta \tau_{3b} \delta_3) - \Gamma_\omega \gamma_0 \omega^0 - \frac{1}{2} \Gamma_\rho \tau_{3b} \gamma_0 \rho^0 - \gamma_0 \Sigma_0^R - \frac{1}{2} \mu_N \kappa_b \sigma_{\mu\nu} F^{\mu\nu} \right) \Psi_b = 0. \quad (32)$$

The effective baryon masses, in this case, are given by

$$m_b^* = m_b - \Gamma_\sigma \sigma - \tau_{3b} \Gamma_\delta \delta_3, \quad (33)$$

and differ for protons and neutrons. In charge-neutral, β -equilibrated matter, the conditions Eq. (12) and Eq. (13) apply.

The energy spectra for protons, neutrons and leptons are given by Eqs. (14), (15) and (16) with the rearrangement term, in this case, given by

$$\Sigma_0^R = \frac{\partial \Gamma_\omega}{\partial \rho} \rho_b \omega_0 + \frac{\partial \Gamma_\rho}{\partial \rho} \rho_3 \frac{\rho_0}{2} - \frac{\partial \Gamma_\sigma}{\partial \rho} \rho^s \sigma + \frac{\partial \Gamma_\delta}{\partial \delta} \rho_3^s \delta_3. \quad (34)$$

The expressions of the scalar and vector densities for protons and neutrons, Fermi momenta, chemical potentials still hold. The energy density of neutron star matter is, now, given by

$$\varepsilon_m = \sum_{b=p,n} \varepsilon_b + \sum_{l=e,\mu} \varepsilon_l + \frac{1}{2} m_\sigma^2 \sigma^2 + \frac{1}{2} m_\omega^2 \omega_0^2 + \frac{1}{2} m_\rho^2 \rho_0^2 + \frac{1}{2} m_\delta^2 \delta_3^2 \quad (35)$$

including an extra term for the δ -meson. For the pressure Eq. (26) holds.

IV. RESULTS AND DISCUSSION

In the present section we discuss the EoS of stellar matter obtained within TW and DDRH δ and compare them with other previously studied models GM3 and TM1. We will pay a special attention to the behaviour of the EoS at subsaturation densities in order to understand how could strong

magnetic fields affect the crust of compact stars by extending or reducing the non-homogeneous phase.

The properties of the isovector channel of the models have an important role on the properties of the EoS of very asymmetric matter and therefore we plot, for reference, in Fig. 1 the symmetry energy of the four models under study. It is seen that the models have quite different behaviours at large densities and this will reflect itself on the EoS. In fact the largest proton fractions occur for the models with the largest symmetry energy since a very asymmetric system will be energetically defavoured. While the DDRH δ is the one with the lower symmetry energy at lower densities, around two times the saturation density its symmetry energy crosses the corresponding curve for the TW. This is due to the saturation of the δ field as discussed in [26]. We may expect that this effect will have influence on the properties of the EoS. GM3 and TM1 have quite high symmetry energy ϵ_{sym} which originates a large proton fraction at subsaturation densities and allows for the direct URCA process. We will see, however that the proton fraction is determined also by the

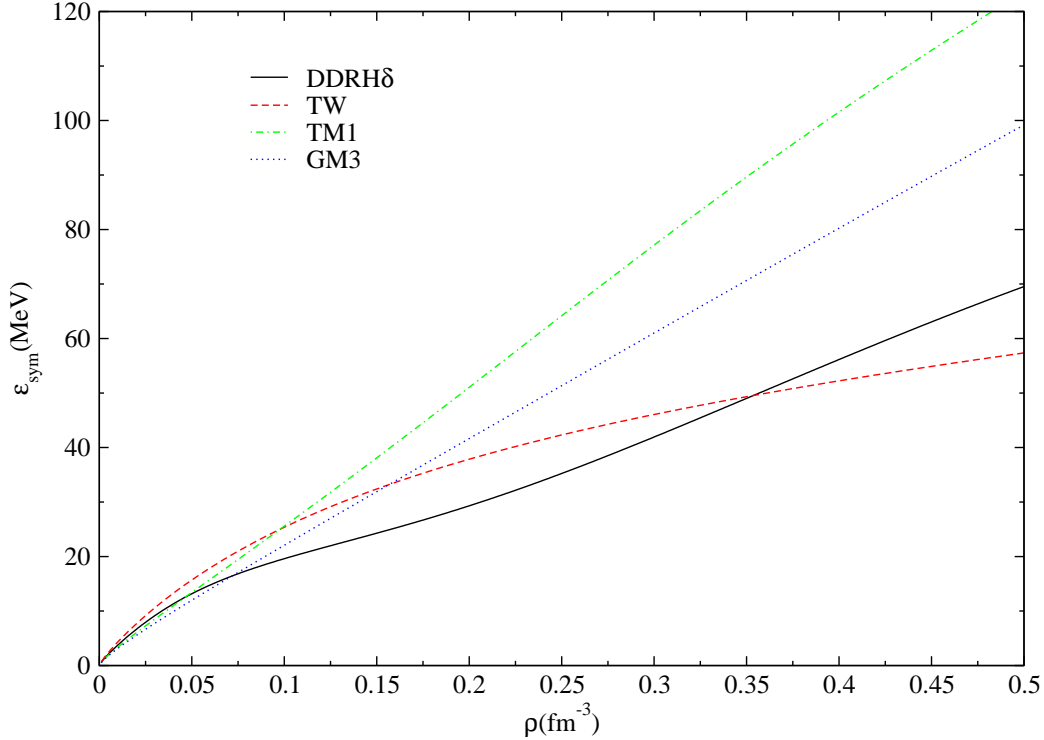


FIG. 1: (Color online) The symmetry energy of the models under study.

magnitude of the effective mass.

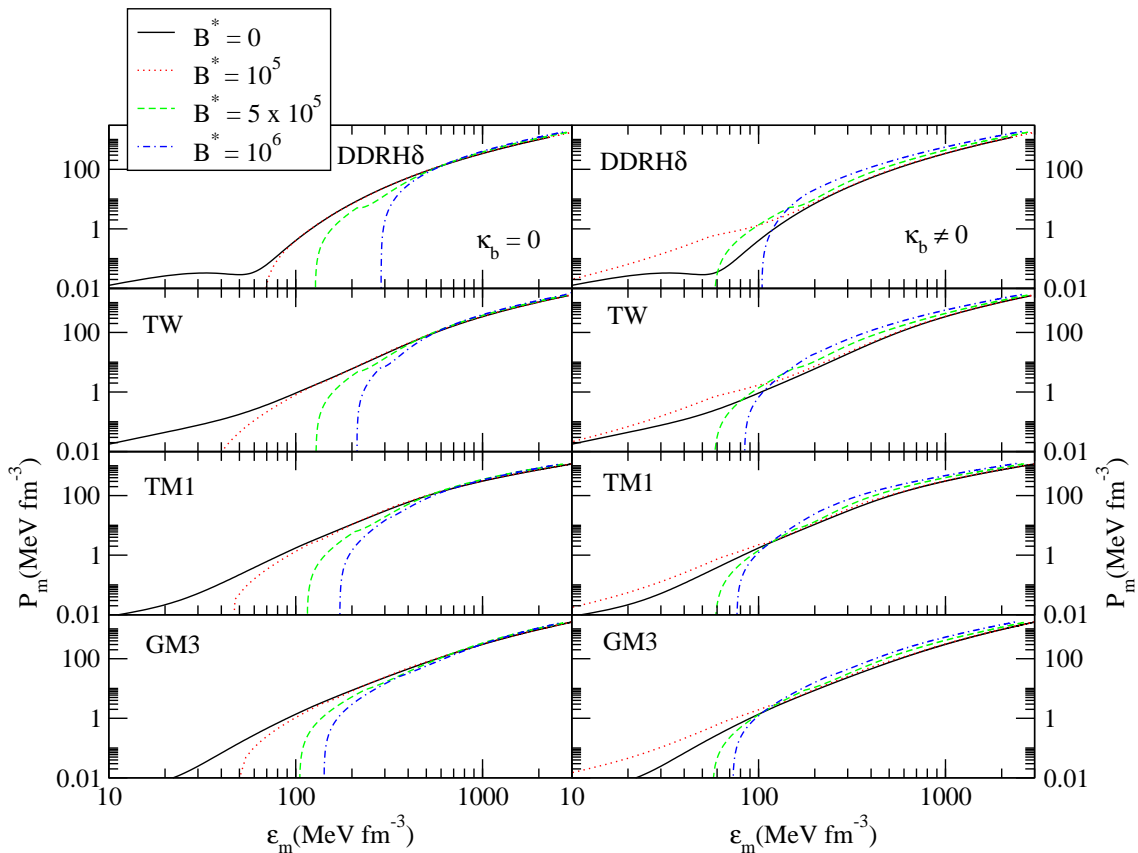


FIG. 2: (Color online) EoS for stellar matter without (left) and with (right) the nucleon anomalous magnetic moment. Several models are considered.

In Fig. 2 we compare the EoS of TM1, GM3, TW and DDRH δ for several magnetic field intensities. As discussed in [8] the magnetic field makes the EoS softer when the anomalous magnetic moment (AMM) of the nucleons is not considered. For $B^* = 10^5$ the strongest effect occurs at low densities typical of the crust of the star. It is therefore important to investigate the influence of the magnetic field on the crust properties. For $B = 0$ it is shown that DDRH δ presents a small liquid-gas phase transition. This is certainly due to the small symmetry energy this model has at low densities. From a qualitative point of view all models behave similarly, also when the AMM is included. In this case the EoS becomes stiffer as the magnetic field increases except for the small densities. In particular the curve for $B^* = 10^6$ gets softer than the $B = 0$ EoS for energy densities smaller than $70 \text{ MeV}/\text{fm}^3$, when the effect of the Landau quantisation is stronger than the AMM contribution.

In order to have a more quantitative comparison, in Fig. 3 we plot for each magnetic field the

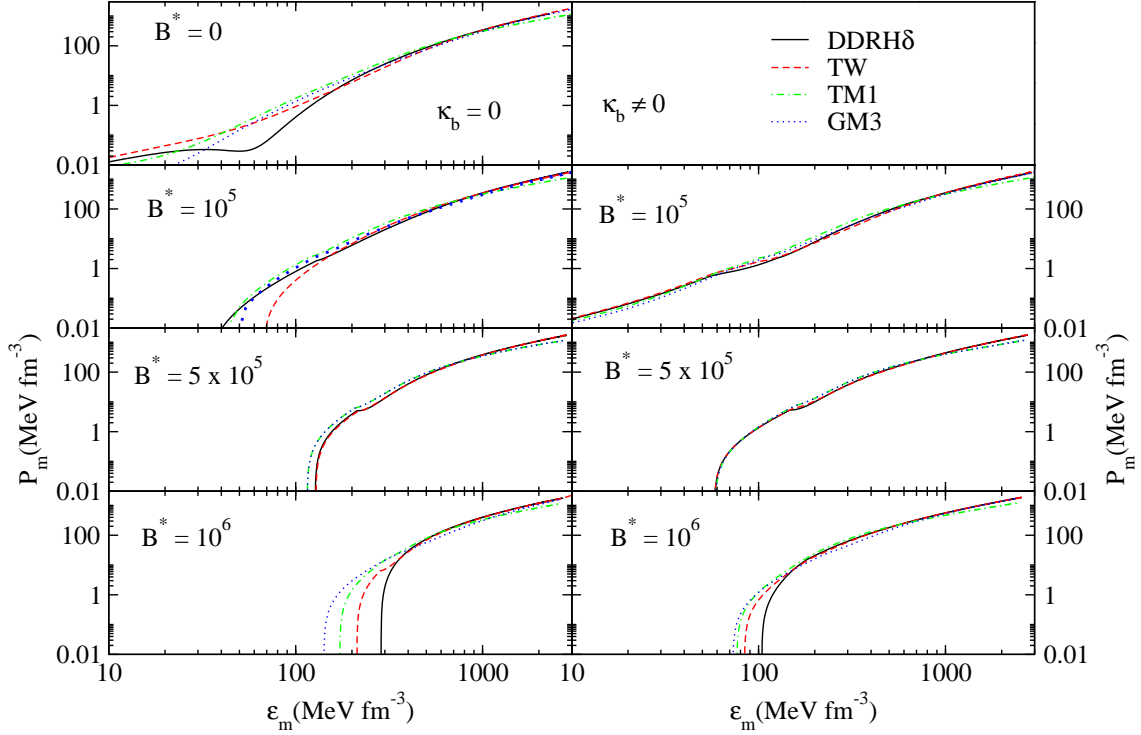


FIG. 3: (Color online) EoS for stellar matter without (left) and with (right) the nucleon anomalous magnetic moment. Several magnetic fields are considered.

four models. If the anomaly is not considered the largest differences occur for the lower densities: at $B = 0$ TM1 and GM3 are the softest at low densities and become the hardest at high densities; DDRH δ is the softest EoS at intermediate energies. The $B = 0$ behaviour is determined by the symmetry energy, and the trend of the EoS follows the relative behaviour of the symmetry energy curves. However the relative stiffness of the EoS depends on the intensity of B . Contrary to the lower values of B^* , 0 and 10^5 , for the highest value GM3 is stiffer than TM1 and for $B^* = 5 \times 10^5$ both EoS have very similar behaviours. Although DDRH δ EoS is softer than the TW EoS below $\epsilon = 200 \text{ MeV}/\text{fm}^3$ for small and large magnetic fields, for $B^* = 10^5$ and 5×10^5 it becomes harder or similar. If the anomaly is included the differences between the models are much smaller mainly for $B^* < 10^6$. For these values, models coincide at intermediate and high densities. For the low densities, differences arise for $B^* \sim 10^6$ or larger.

In Fig. 4 only the region $\rho < 1.5\rho_0$ is plotted. The magnetic field increases the binding at

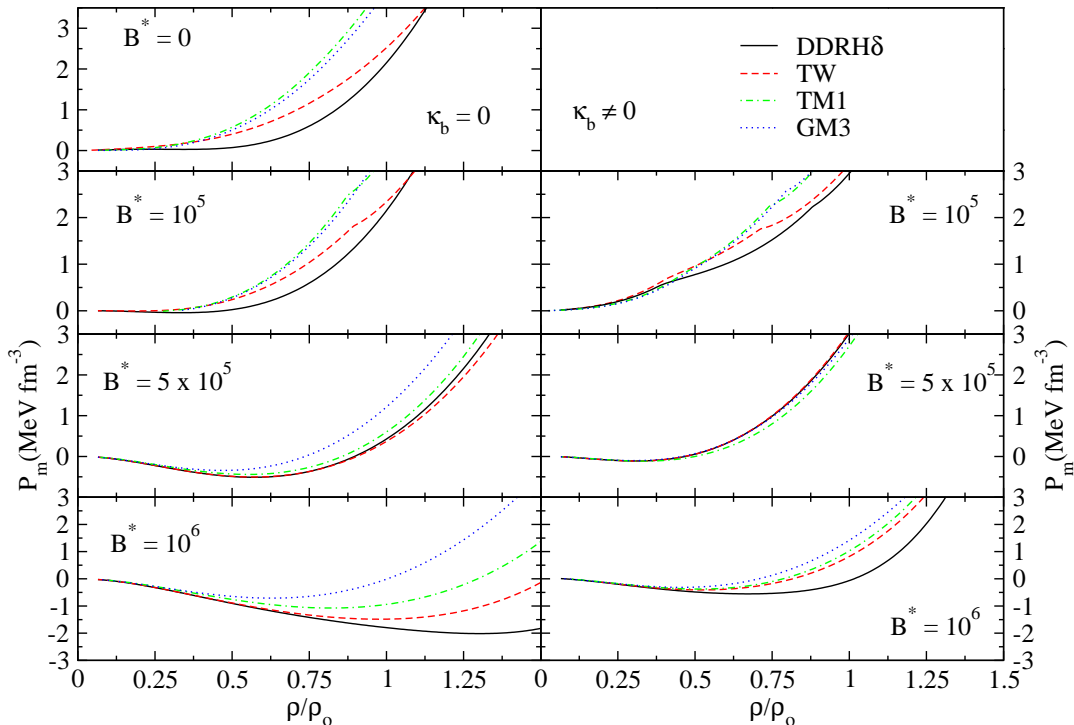


FIG. 4: (Color online) EoS at low densities for stellar matter without (left) and with (right) the nucleon anomalous magnetic moment. Several magnetic fields are considered.

low densities and a negative pressure may still occur beyond $2\rho_0$. The most bound matter occurs for DDRH δ and this is due to the low symmetry energy this model has at intermediate densities. This means that the crust extends itself to higher densities and a higher value of the density will characterise the inner edge of the crust. The inclusion of the AMM reduces this effect but binding still occurs and there are also regions of negative compressibility and/or pressure defining an unstable region. It is clearly seen that the models behave differently in these range of densities when the B field increases. GM3 becomes harder than TM1 for $B^* > 5 \times 10^5$. Also the relative behavior of TW and DDRH δ change.

In order to better understand the low density behavior we have determined the upper density limit of the mechanical instability, the density at which the incompressibility becomes zero, as a function of the magnetic field, Fig. 5a), and calculated the associated proton fraction Fig. 5b). For β -equilibrium nuclear matter with no magnetic field there are no mechanical instabilities even if

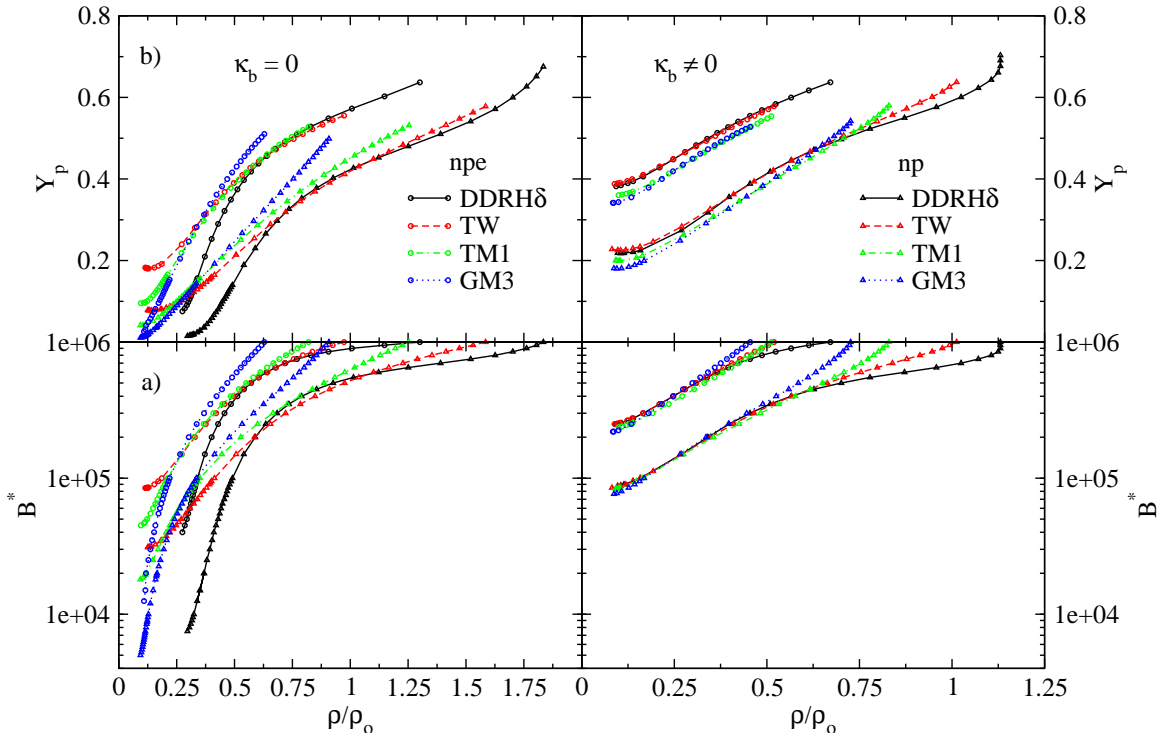


FIG. 5: (Color online) Low density mechanical instability. Bottom: The upper limit of the mechanical instability for different magnetic fields as a function of density; top: the corresponding proton fraction; left: no AMM; right: including AMM.

we only consider neutron-proton (np) matter and do not add the electron contribution, for which the incompressibility is always positive. In Table II we give the densities for which the EoS for β -equilibrium matter at a zero magnetic field crosses the thermodynamical spinodal for np matter. As shown in [37] these numbers give an order of magnitude of the upper limit of the transition density: neither the Coulomb force nor the finite range of the nuclear force is taken into account. They are slightly larger than the corresponding values obtained from the crossing of the dynamical spinodal with the EOS for neutron-proton-electron (npe) matter, which define a lower limit, and of the same order of magnitude of the results obtained from the transition of a pasta phase to a homogeneous phase [37].

From Fig. 5 we see that the magnetic field, if strong enough, may change this picture, more strongly if the AMM is not considered. In this figure we show both the mechanical instability upper bound for np matter and also for npe matter. Of course in the last case the instability region is

TABLE II: Predicted density and pressure at the inner edge of the crust of a compact star at zero temperature, as defined by the crossing between the thermodynamical instability region of np matter and the β -equilibrium condition for homogeneous, neutrino-free stellar matter.

	$\rho_b(\text{fm}^{-3})$	$P_m(\text{MeVfm}^{-3})$
TM1	0.069509	0.50288
GM3	0.068762	0.35644
TW	0.084955	0.52246
DDRH δ	0.085038	0.12855

smaller due to the high incompressibility of the electron gas and occurs at larger proton fraction when the symmetry term contribution is smaller. The existence of a mechanical instability region in the presence of the magnetic field has two reasons: a) due to the existence of Landau levels the nucleonic pressure does not increase so fast with density and b) at large magnetic fields the proton fraction increases and the symmetry repulsive term in the energy density is not so strong. The model DDRH δ is the one showing the largest instability ranges and at least, for the no AMM calculation, it also predicts the smaller proton fractions. However, when the AMM contribution is introduced the proton fraction of all models behave in a very similar way except for the larger fields. In fact we should perform a calculation which includes the Coulomb interaction and surface energy, but according to studies done in [21, 38, 39], the spinodal which includes these effects would be larger than the mechanical instability region we have calculated. A complete study of the low density region, namely the spinodal surface that limits the non-homogeneous phase, needs to be done.

The fraction of protons and muons for the models and field intensities discussed are given in Fig. 6 as a function of density. For comparison we also include the $B = 0$ results. The effect of the magnetic field is not very large for $B^* = 10^5$, except at low densities, $\rho < 2\rho_0$, when protons are totally polarised. In Fig. 7a) we show the occupied Landau levels as a function of density and in Fig. 7b) the neutron polarization for the calculation including AMM. For $B^* = 10^5$ ($B^* = 5 \times 10^5$) the second Landau level starts being occupied only for densities above $\sim 2\rho_0$ ($\sim 8\rho_0$). GM3 has a similar behaviour to TM1 and DDRH δ an intermediate behaviour between TM1 and TW. From Fig. 7b) we conclude that while at $B^* = 10^5$ neutrons are only slightly polarized at $B^* = 10^6$ they are totally polarized for densities below $8\rho_0$. This total neutron polarization favours an increase of the proton fraction when AMM is included.

The fraction of protons within the different models is determined by the symmetry energy of

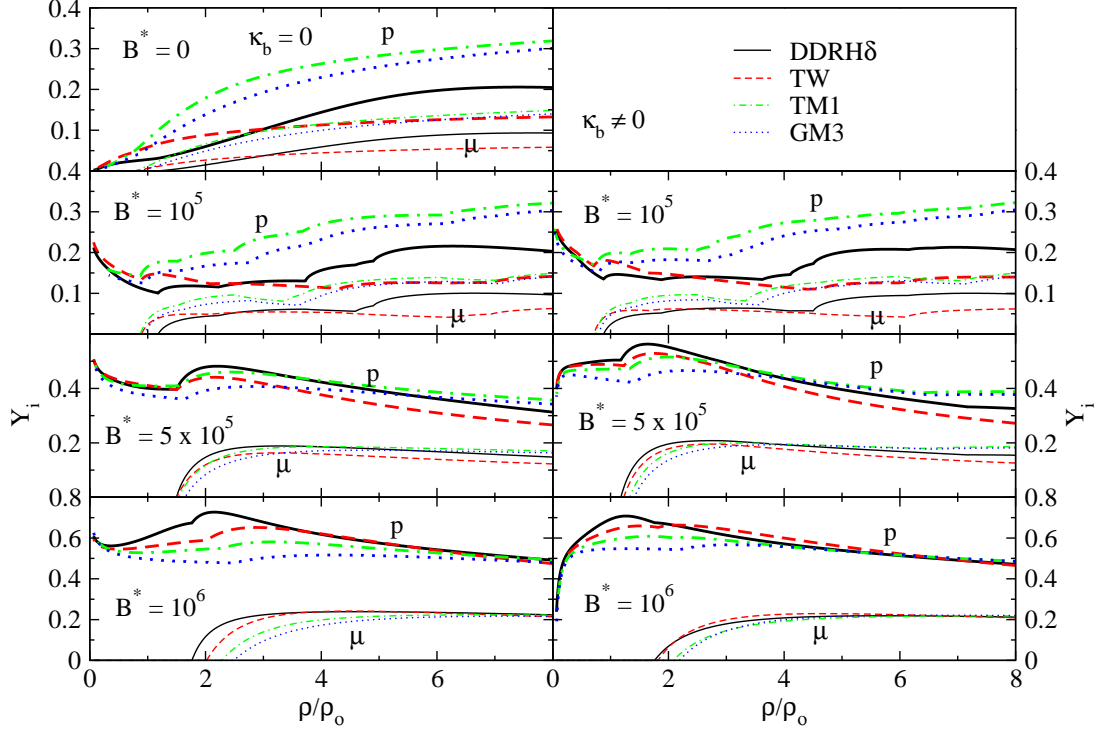


FIG. 6: (Color online) Proton and muon fraction for stellar matter without (left) and with (right) the nucleon anomalous magnetic moment. Several magnetic fields are considered.

the respective model for the density considered. This explains why for $B^* \leq 10^5$, DDRH δ has the smallest fraction for $\rho < 2.5\rho_0$. For $\rho > 2.5\rho_0$ it is TW which has the smallest symmetry energy and the smallest proton fraction. For high fields, $B^* > 10^6$ the fraction of protons is larger than the fraction of neutrons and again the symmetry energy defines the models with the largest fraction: DDRH δ for $\rho < 3\rho_0$ and TW for densities larger than $3\rho_0$. At $B^* = 5 \times 10^5$ all proton fraction lie between 0.4 and 0.5 for densities below $4\rho_0$. The relative fraction of protons is then determined by the effective mass: GM3 has the lower fraction due to its larger mass. On the other hand DDRH δ has the smallest proton mass a largest proton fraction. This effect is even larger for $B^* = 10^6$. The inclusion of the AMM has important effects for $B^* > 10^6$. For densities $\rho < 2\rho_0$ the behaviour of the different models is still distinguishable but for larger densities the behaviour of all models is mostly determined by the magnetic field intensity. The magnetic field gives rise to an onset of muons at larger densities when the anomaly is not included because the magnetic fields favours a

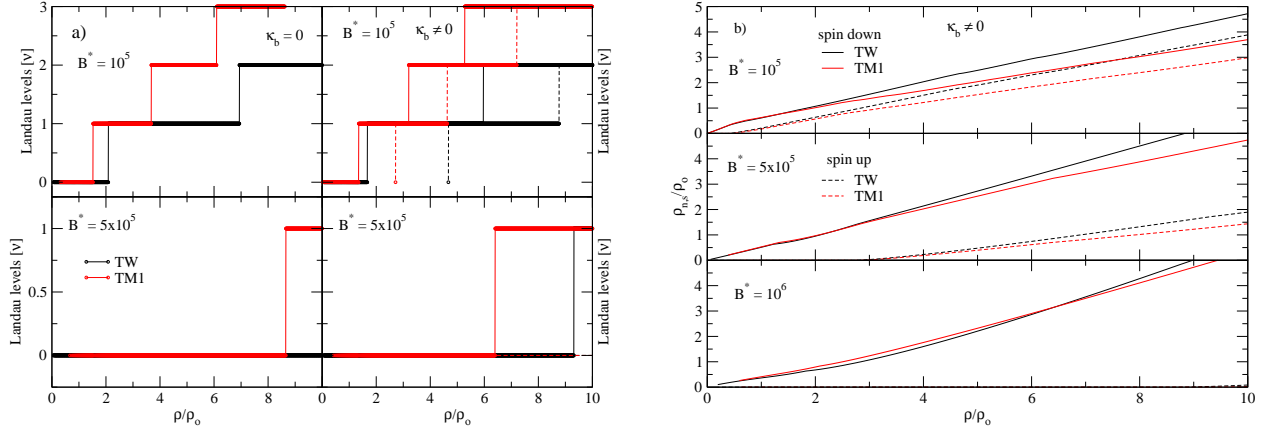


FIG. 7: (Color online) Density dependence of the proton and neutron polarization for TM1 and TW and different values of the magnetic field: a) Landau levels occupied by protons without (left) with (right) AMM. The dashed lines indicate the onset of spin down for each Landau level in the calculation with AMM; b) neutron polarization, full (dashed) lines correspond to spin down (up).

larger proton fraction and therefore a smaller electron chemical potential. With the introduction of the AMM, the electron chemical potential increases slightly which explains the onset of muons at lower densities.

In Fig. 8 the effective mass of the nucleons within the models under study are shown as a function of the density for different intensities of the magnetic field, with and without the AMM. As discussed in [8] when the AMM is not taken into account and the magnetic field becomes more intense, the effective mass reduces faster with an increase of the density. For $B^* = 10^5$ the effect of the magnetic field is still small, but for larger values it becomes more important. For $B^* = 10^5$ there is total polarisation only for $\rho < 2\rho_0$ while for $B^* = 10^6$ there is total polarisation for the all range of densities considered. The GM3 model has the largest mass for all fields considered. At saturation and without magnetic field this model predicts an effective mass of $0.78 M$ while for all the others the effective mass at saturation is $0.6 M$ or smaller. The large values of the effective mass within GM3 justify the smaller proton fractions for the most intense magnetic fields. On the order hand DDRH δ shows the fastest reduction of the effective mass with density. For DDRH δ we show both the proton and the neutron mass. In this model, the mass of the most abundant nucleon, neutron for $B^* = 10^5$, 0.5×10^6 and proton for $B^* = 10^6$, or larger, behaves like the nucleon mass in all the other models (except GM3), having slightly smaller values. The mass of the less abundant nucleon is quite higher, similar to the nucleon mass in GM3 for the smaller

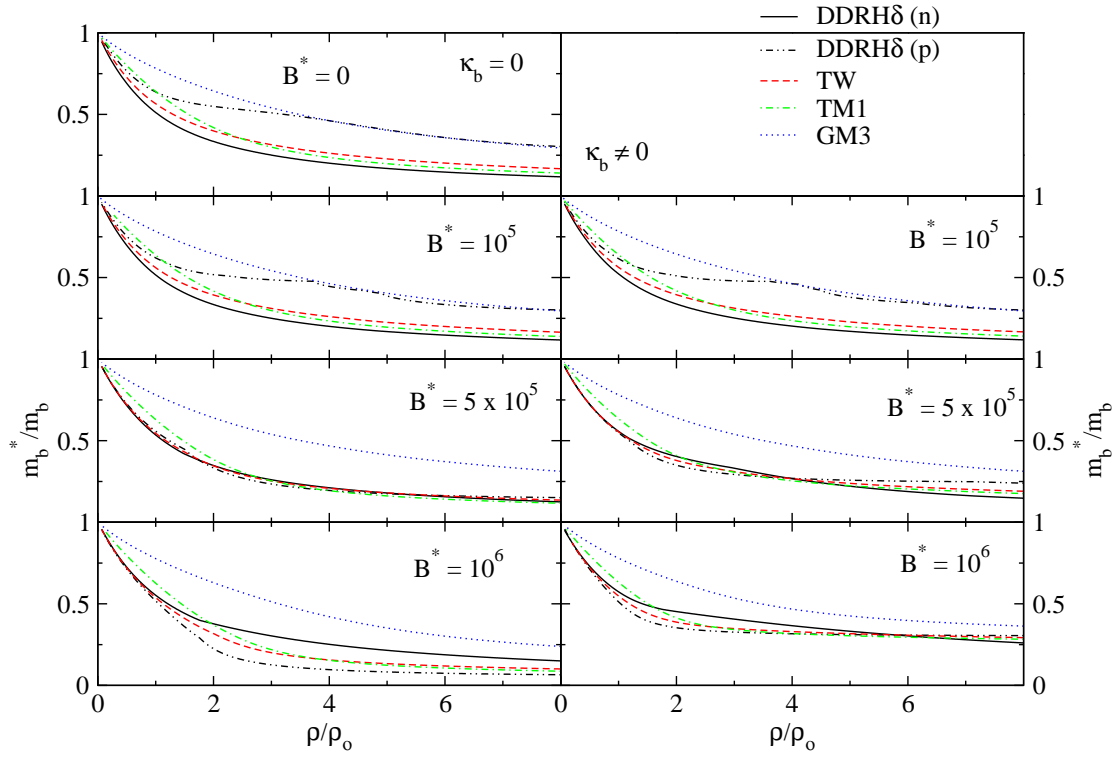


FIG. 8: (Color online) Nucleon effective mass for stellar matter without (left) and with (right) the nucleon anomalous magnetic moment.

magnetic fields. If the AMM is included the effective masses saturate quite fast at a non-zero value which corresponds to $m_b - s\mu_N\kappa_i B$, $i = p, n$. Models with density dependent couplings saturate faster than the other two.

The behaviour of the nucleon masses is better understood from the behaviour of the scalar field with density. In Fig. 9 we plot the σ and δ fields, more precisely $\Gamma_\sigma\sigma$ and $-\Gamma_\delta\delta_3$ as a function of the density for several magnetic field intensities. If the AMM is not included the δ -field changes sign for the two most intensive fields considered. This reflects the existence of a larger fraction of protons than neutrons. The inclusion of AMM reduces this effect and only for a restricted range of densities below $3 - 4\rho_0$. This is due to the larger effective mass of the protons. We also see that the σ field increases faster with density for the larger magnetic fields, giving rise to a faster saturation of the effective mass. If the AMM is taken into account the saturation of σ field does not occur at the baryonic mass value but at the value of the renormalised baryonic mass by the

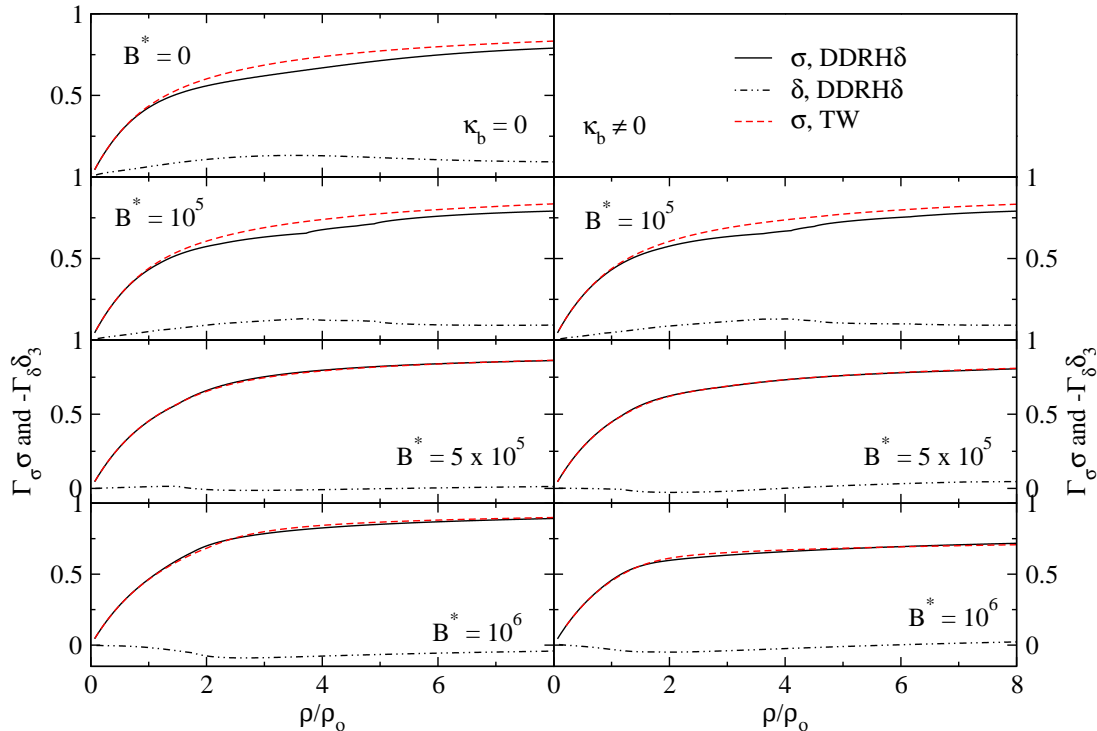


FIG. 9: (Color online) The σ and δ -fields for stellar matter without (left) and with (right) the nucleon anomalous magnetic moment.

AMM, see Eq. (21).

V. CONCLUSIONS AND OUTLOOKS

In the present paper we have compared the EoS for stellar matter made out of protons, neutrons, electrons and muons in the presence of very strong magnetic fields. In particular, we have studied the EoS obtained within DDRH models with and without the scalar-isovector meson δ and compared with other models previously studied: GM3 and TM1.

It has been shown that, although the overall behaviour of all the models is similar, at low densities, $\rho < 3\rho_0$, the models show the largest differences. In particular, it has been shown that the low density instability region increases a lot as the magnetic field increases when the AMM is not taken into account. Although the AMM reduces this behaviour there remains a region of instability not present for the magnetic field free matter. The larger range of instability is partially

due to the larger proton fractions and partially due to the appearance of Landau levels.

Moreover DDRH δ model shows a low density instability, which will give rise to a liquid-gas phase transition, even for $B = 0$. This could be due to the low symmetry energy it has at low and intermediate densities. It is also the DDRH δ model that shows the largest changes of behaviour with the magnetic field and the density, both due to the presence of the δ -meson and the density dependence of the coupling parameters. This is particularly clear with the EoS and the proton and muon fractions. In fact, the DDRH models are the ones that predict smaller (higher) proton fractions at intermediate densities for $B^* \leq 10^5$ ($B^* \geq 10^6$), reflecting the behaviour of the symmetry energy, the proton effective mass with density and the difference between proton and neutron masses. Although the EoS of the different models do not differ so much, properties of the star sensitive to the proton fraction will distinguish the different models. These may be the neutrino interaction with hadronic matter, it is larger for larger neutron fractions, or the pairing properties of stellar matter which affect neutrino emissivities and specific heat. The stars more sensitive to the differences between the models are the low mass ones with $M \sim 1.0M_{\odot}$. In particular, we have shown that the proton-neutron mass spitting present in DDR δ parametrization has noticeable effects on the proton fractions predicted by this model, changing at intermediate densities from the smallest ones to the largest ones.

In the present study we have not considered strangeness. At large densities about two times the saturation density we may expect the onset of hyperons [2], or kaon condensation [40]. The effect of strong magnetic fields on the onset of strangeness has been discussed in [41, 42] and it was shown that both the hyperon or the kaon condensate onset occurs at larger densities, $> 5\rho_0$, in the presence of strong fields. So we may consider in the present discussion that results will not be affected by the strangeness degree of freedom below $5\rho_0$. It remains, however to be checked if the density dependence of the baryon-meson couplings will have an effect on the hyperon onset.

The study of the effect of the magnetic field on the low density instabilities is of particular interest: the way the clusterization occurs and the extension of the crust will affect the cooling and conduction properties of the star. It was shown in the present work that the properties of the crust under strong magnetic fields are sensitive to the EoS used. A detailed study of the effect of strong magnetic fields on the low density instabilities of nuclear matter is being carried on.

Acknowledgments

This work was partially supported by FEDER and FCT (Portugal) under the grant SFRH/BPD/14831/2003, and projects POCI/FP/81923/2007 and PDCT/FP/64707/2006. A. R. specially acknowledges many useful and elucidating discussions with A. M. Santos.

-
- [1] B. D. Serot and J.D. Walecka, *Adv. Nucl. Phys.* 16, 1 (1986); J. Boguta and A. R. Bodmer, *Nucl. Phys.* A292, 413 (1977).
 - [2] N. K. Glendenning, *Compact Stars*, Springer-Verlag, New-York, 2000.
 - [3] T. Klähn et al., *Phys. Rev. C* 74, 035802 (2006).
 - [4] R. C. Duncan and C. Thompson, *Astrophys. J.* 392, L9 (1992); C. Thompson and R. C. Duncan, *MNRAS* 275, 255 (1995).
 - [5] V. V. Usov, *Nature* 357, 472 (1992).
 - [6] B. Paczyński, *Acta Astron.* 42, 145 (1992).
 - [7] A. K. Harding and D. Lai, *Rep. Prog. Phys.* 69, 2631 (2006).
 - [8] A. Broderick, M. Prakash, and J. M. Lattimer, *Astrophys. J.* 537, 351 (2000).
 - [9] S. Chakrabarty, *Phys. Rev. D* 54, 1306 (1996); S. Chakrabarty, D. Bandyopadhyay, and S. Pal, *Phys. Rev. Lett.* 78, 2898 (1997).
 - [10] Deborah N. Aguilera, José A. Pons, Juan A. Miralles, astro-ph/0710.0854
 - [11] SGR/APX online Catalogue, <http://www.physics.mcgill.ca/~pulsar/magnetar/main.html>
 - [12] C. Fuchs, H. Lenske, and H. H. Wolter, *Phys. Rev. C* 52, 3043 (1995).
 - [13] S. Typel and H. H. Wolter, *Nucl. Phys. A* 656, 331 (1999).
 - [14] R. Brockmann and R. Machleidt, *Phys. Rev. C* 42, 1965 (1990); S. Haddad and M. Weigel, *Phys. Rev. C* 48, 2740 (1992); F. de Jong and H. Lenske, *Phys. Rev. C* 57, 3099 (1998).
 - [15] E. Chabanat, P. Bonche, P. Haensel, J. Meyer and R. Schaeffer, *Nucl. Phys. A* 627, 710 (1997)
 - [16] A.W. Steiner, M. Prakash, J.M. Lattimer and P.J. Ellis, *Phys. Rep.* 411, 325 (2005).
 - [17] A. Akmal, V. R. Pandharipande, and D. G. Ravenhall, *Phys. Rev. C* 58, 1804 (1998).
 - [18] H. S. Xu et al., *Phys. Rev. Lett.* 85, 716 (2000).
 - [19] C. Providência, *Int. J. Mod. Phys. E* 16, 2780 (2007).
 - [20] A. S. Santos, L. Brito, and C. Providência, *Phys. Rev. C* 77, 045805 (2008).
 - [21] S. S. Avancini, L. Brito, Ph. Chomaz, D. P. Menezes, and C. Providência, *Phys. Rev. C* 74, 024317 (2006).
 - [22] M. Dutra, O. Lourenço, A. Delfino, J.S. Sá Martins, C. Providência, S. S. Avancini, and D. P. Menezes, *Phys. Rev C* 77, 035201 (2008).
 - [23] P. Yue and H. Shen, *Phys. Rev. C* 74, 045807 (2006).

- [24] Y. F. Yuan and J. L. Zhang, *ApJ*, 525, 950, (1999); G.-J. Mao, A. Iwamoto and Z.-X. Li, *Chin. J. Astron. Astrophys.* Vol.3, No 4, 359-374 (2003).
- [25] S. Kubis and M. Kutschera, *Phys. Lett. B*399, 191 (1997)
- [26] B. Liu, V. Greco, V. Baran, M. Colonna, and M. Di Toro, *Phys. Rev. C* 65, 045201 (2002).
- [27] Debora P. Menezes and C. Providência, *Phys. Rev. C* 70, 058801 (2004).
- [28] L. Brito, Ph. Chomaz, D. P. Menezes and C. Providência, *Phys. Rev. C* 76, 044316 (2007).
- [29] V. Baran, M. Colonna, V. Greco and M. di Toro, *Phys. Rep.* 410,335 (2005).
- [30] Lie-Wen Chen, Che Ming Ko and Bao-An Li, *Phys. Rev. C*76, 054316 (2007)
- [31] P. Finelli, N. Kaiser, D. Vretenar and W. Weise, *Nucl. Phys. A*770, 1 (2006)
- [32] T. Gaitanos, M. Di Toro, S. Typel, V. Baran, C. Fuchs, V. Greco, and H. H. Wolter, *Nucl. Phys. A*732, 24 (2004).
- [33] N. K. Glendenning and S. A. Moszkowski, *Phys. Rev. Lett.* 67, 2414 (1991).
- [34] Y. Sugahara and H. Toki, *Prog. Theor. Phys.* 92, 803 (1994).
- [35] G. Hua, L. Bo, and M. Di Toro, *Phys. Rev. C* 62, 035203 (2000).
- [36] S. S. Avancini, L. Brito, D. P. Menezes, and C. Providência, *Phys. Rev. C* 70, 015203 (2004).
- [37] S.S. Avancini, D.P. Menezes, M.D. Alloy, J.R. Marinelli, M.M.W. Moraes, C. Providência, *Phys. Rev. C* 78, 015802 (2008).
- [38] Horst Müller and Brian D. Serot, *Phys. Rev. C* 52, 2072 (1995)
- [39] C. Providência, L. Brito, S.S. Avancini, D. P. Menezes and Ph. Chomaz, *Phys. Rev. C* 73, 025805 (2006).
- [40] N. K. Glendenning and J. Schaffner-Bielich, *Phys. Rev. C* 60, 025803 (1999).
- [41] A. Broderick, M. Prakash, and J. M. Lattimer, *Phys. Lett. B* 531, 167 (2002).
- [42] P. Dey, A. Bhattacharyya, and D. Bandyopadhyay, *J. Phys. G* 28, 2179 (2002).